Molecular keys of the tropism of integration of the cholera toxin phage

Bhabatosh Das, Julien Bischerour, Marie-Eve Val, François-Xavier Barre

Molecular keys of the tropism of integration of the cholera toxin phage

Bhabatosh Das[a,b,1], Julien Bischerour[a,b,1], Marie-Eve Val[a,b], and François-Xavier Barre[a,b,2]

[a]Centre de Génétique Moléculaire, Centre National de la Recherche Scientifique, 91198 Gif-sur-Yvette, France; and [b]Université Paris-Sud, 91405 Orsay, France

Edited by G. Balakrish Nair, National Institute of Cholera and Enteric Diseases, Kolkata, India, and approved December 22, 2009 (received for review September 7, 2009)

Cholera toxin is encoded in the genome of CTXϕ, a lysogenic filamentous phage of *Vibrio cholerae*. CTXϕ variants contribute to the genetic diversity of cholera epidemic strains. It has been shown that the El Tor variant of CTXϕ hijacks XerC and XerD, two host-encoded tyrosine recombinases that normally function to resolve chromosome dimers, to integrate at *dif*1, the dimer resolution site of the larger of the two *V. cholerae* chromosomes. However, the exact mechanism of integration of CTXϕ and the rules governing its integration remained puzzling, with phage variants integrated at either or both dimer resolution sites of the two *V. cholerae* chromosomes. We designed a genetic system to determine experimentally the tropism of integration of CTXϕ and thus define rules of compatibility between phage variants and dimer resolution sites. We then showed in vitro how these rules are explained by the direct integration of the single-stranded phage genome into the double-stranded bacterial genome. Finally, we showed how the evolution of phage attachment and chromosome dimer resolution sites contributes to the generation of genetic diversity among cholera epidemic strains.

lysogenic conversion | site-specific recombination

Cholera toxin, which is responsible for the deadly diarrhea associated with the disease of the same name, is one of the most significant virulence factors of *Vibrio cholerae* (1). It is encoded in the genome of a lysogenic filamentous bacteriophage, CTXϕ (2). Different CTXϕ variants exist, the two main ones being classified as "classical" and "El Tor," according to the biotype of the hosts in which they originally were identified (Fig. 1*A*) (3). The existence of several different CTXϕ variants and their integration in variable copy numbers on the first, the second, or both *V. cholerae* chromosomes contribute to the genetic diversity of cholera epidemic strains (Fig. 1*A*) (4).

In contrast to most other lysogenic phages, such as phage λ, CTXϕ does not encode its own integration machinery. Instead, it has been shown that the El Tor variant of CTXϕ hijacks XerC and XerD, two host-encoded tyrosine recombinases that normally function to resolve chromosome dimers (5), to integrate at *dif*1, the dimer resolution site of the larger of the two *V. cholerae* chromosomes (6). Xer recombination sites consist of binding sites for XerC and XerD, separated by a 6-bp to 8-bp overlap region; strand exchanges occur at the border of this region (7). The replicative form of CTXϕ harbors two putative Xer recombination sites in inverted orientations, *att*P1 and *att*P2 (pCTXϕ; Fig. 1*B*). This observation led to the proposal of two integration models (8, 9). The first model predicts that recombination occurs between *dif*1 and *att*P1 as the result of an unknown architectural function played by *att*P2. The second model relies on the formation of a forked hairpin by the ~150-bp region encompassing *att*P1 and *att*P2 in the (+) ssDNA genome of the phage, which unmasks a putative phage attachment site, *attP*(+) [CTXϕ (+) ssDNA; Fig. 1*B*]. Both models rely on the exchange of a single pair of strands catalyzed by XerC and on the conversion of the resulting Holliday junction into product by repair and/or replication.

According to both models, no integration should occur at *dif*2, the dimer resolution site of the second *V. cholerae* chromosome, because no Watson–Crick bp interactions could stabilize the exchange of strands catalyzed by XerC (Fig. 1*C*). Nevertheless, the classical variant of CTXϕ was found integrated at *dif*2 in classical strains (3) and in recent El Tor isolates (4, 10–14). The mode of dissemination of this variant is of particular interest, because it allows the production of an elevated amount of cholera toxin (15, 16) that seems to be implicated in a high proportion of severe infections associated with classical strains (17). It was proposed that this variant recently invaded the genome of El Tor strains through chitin-induced competence and homologous recombination (18). However, the transformation efficiency was very low, in the order of 10^{-6} to 10^{-4}. In addition, such a mechanism does not explain how CTXϕ initially achieved *dif*2 integration or the diversity of combinations of the different genetic elements that were found integrated at the two chromosome dimer resolution sites of *V. cholerae* strains (4).

In this study, we designed a sensitive assay to monitor the efficiency with which CTXϕ integrates at *dif*1 and *dif*2 in *V. cholerae*. Using this assay, we demonstrated the specificity of integration of the El Tor variant of CTXϕ harbored by strain N16961. In contrast, the classical variant of CTXϕ harbored by strain 569B efficiently integrated at both *dif*1 and *dif*2. We found that the altered integration behavior of the classical phage is caused by two base changes in the overlap region of *att*P2 that allow *V. cholerae* XerCD to recombine the classical ssDNA *att*P(+) region with *dif*1 and *dif*2 in vitro. These results further support the ssDNA integration model and allow the definition of rules of compatibility between phage attachment and dimer resolution sites that explain the tropism of integration of the different CTXϕ variants. Based on these rules, we designed a phage attachment site that exclusively targets *dif2*. We also explained how O1 and O139 *V. cholerae* strains with altered dimer resolution sites can escape lysogenic conversion by the most common variants of CTXϕ and showed how a new variant of CTXϕ has evolved that can integrate into the genome of these particular strains. Taken together, these results suggest that lysogenic conversion by CTXϕ is the primary mode of acquisition of the cholera toxin genes, which, along with the evolution of phage attachment and chromosome dimer resolution sites, contributes to the generation of genetic diversity among cholera epidemic strains.

Author contributions: B.D., J.B. and F.-X.B. designed research; B.D. and J.B. performed research; M.-E.V. contributed new reagents/analytic tools; B.D., J.B. and F.-X.B. analyzed data and wrote the paper.

The authors declare no conflict of interest.

This article is a PNAS Direct Submission.

See Commentary on page 3951.

[1]B.D. and J.B. contributed equally to this work.

[2]To whom correspondence should be addressed. E-mail: barre@cgm.cnrs-gif.fr.

This article contains supporting information online awww.pnas.org/cgi/content/full/0910212107/DCSupplemental.

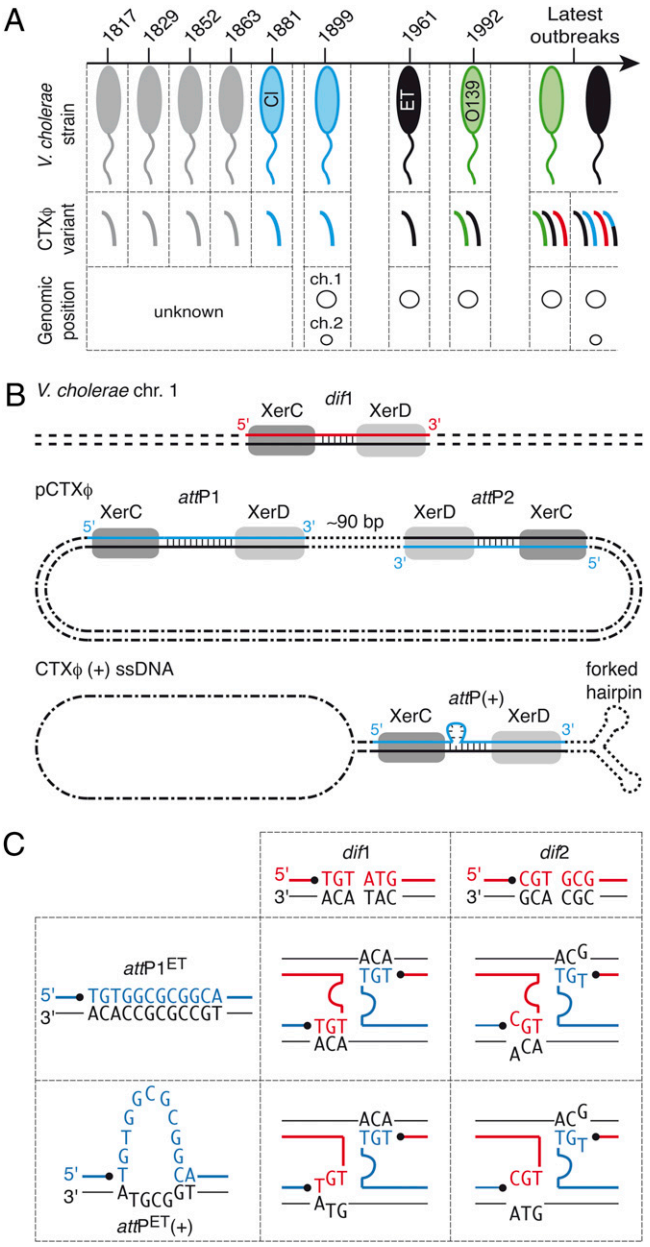

Fig. 1. Lysogenic conversion of *V. cholerae* strains by CTXϕ. (*A*) CTXϕ variants found in cholera epidemic strains. *V. cholerae* strains: gray, unknown; blue, classical; black, El Tor; green, O139. CTXϕ variants: gray, unknown; blue, classical; black, El Tor; green, O139; red, G; black and blue, El Tor and classical hybrid. (*B*) Scheme of Xer recombination sites. *dif*1, dimer resolution site of the N16961 chromosome 1; *att*P1 and *att*P2, Xer sites found in the replicative form of CTXϕ (pCTXϕ); *att*P(+), the recombination site created by the folding of the (+) ssDNA genome of CTXϕ. The two DNA strands of each site are drawn. The strand cleaved by XerC is shown in color. Vertical bars indicate bases present in the overlap region of each site. (*C*) Schemes of the Watson–Crick bp interactions that could stabilize the strand exchange catalyzed by XerC between the overlap regions of the two chromosome dimer resolution sites of N16961 and the two putative attachment sites of El Tor variants of CTXϕ. *dif*1, chromosome 1 dimer resolution site; *dif*2, chromosome 2 dimer resolution site; *att*P1^{ET}, *att*P1 found in CTXϕ El Tor variants; *att*P(+)^{ET}, attachment site unmasked by the folding of the (+) ssDNA genome of El Tor variants of CTXϕ. The strands cleaved by XerC on dimer resolution and phage attachment sites are shown in red and in blue, respectively. Pairing interactions are indicated by the proximity of the bases.

Results

Design of a Sensitive Assay to Monitor the Efficiency and Specificity of CTXϕ Integration. Previous studies that addressed the mechanism of integration of CTXϕ used Southern and PCR techniques to determine the location of each integration event. These techniques are robust. However, because the integration of CTXϕ at *dif*2 might be a very rare event, we sought to design a time- and cost-effective method to monitor its frequency of occurrence. To this aim, we inserted *dif*2 in the coding region of the *Escherichia coli lacZ* gene in such a manner that the produced peptide might retain its β-galactosidase activity. We then engineered an N16961 El Tor strain in which the endogenous *lacZ* gene was deleted and in which *dif*2 was replaced by the *lacZ*::*dif*2 allele (Table 1). These cells turn blue in the presence of X-gal because the β-galactosidase they produce is active. *dif*2 integration events disrupt the *lacZ* ORF, thereby abolishing β-galactosidase production. Thus we could screen for such events simply by plating cells on X-gal media.

The two chromosomes harbored by classical strains possess the same *dif*2 dimer resolution site (CP000626.1). This situation could have favored *dif*2 integration because of the absence of the preferential attachment site of CTXϕ in the bacterial genome. To mimic this situation, we used as a background for our assays an N16961 El Tor strain in which *dif*1 and the integrated copies of CTXϕ surrounding it had been deleted (Table S1). Finally, we engineered a *lacZ*$^{-}$/*dif*2^{-} N16961 El Tor strain in which *dif*1 was replaced by a functional *E. coli lacZ*::*dif*1 gene to monitor the efficiency with which CTXϕ integrates at *dif*1 (Table S1).

The Variant of CTXϕ Found in the 569B Classical Strain Integrates at Both *dif*1 and *dif*2. Studies of the mechanism of integration of the classical variant of CTXϕ were complicated because no phage production was observed in any of the strains harboring it (3, 11). To circumvent this difficulty, we used conjugation to deliver circular DNA molecules carrying the replication and integration region of the phage found in the 569B classical strain, hereafter referred to as "RS^{Cl}," directly into *V. cholerae* cells. To this aim, we cloned RS^{Cl} in a conjugative vector that carries a chloramphenical resistance gene but cannot replicate autonomously in *V. cholerae* (Table S2). We also cloned the replication and integration region of RS1, a truncated derivative of CTXϕ found in the N16961 El Tor strain (19), hereafter referred to as "RS^{ET}" (Table S2). The attachment site of RS1 is identical to the attachment site of the El Tor variants of CTXϕ. In addition, RS1 efficiently and specifically integrates at *dif*1, making it a perfect control for our experiments. Conjugation of the RS^{ET} and RS^{Cl} vectors gave rise to similar numbers of Cm^{R} colonies. RS^{ET} integrated in 100% of the colonies of *dif*1^{+}/*dif*2^{-} cells and in no colonies of *dif*1^{-}/*dif*2^{+} cells, confirming its highly specific integration at *dif*1 (Table 1). In contrast, RS^{Cl} integrated in 36.4% of the colonies of *dif*1^{+}/*dif*2^{-} cells and in 4% of the colonies of *dif*1^{-}/*dif*2^{+} cells, indicating that it efficiently targets both *dif*1 and *dif*2 (Table 1). The integration specificity was not linked to the genomic context of the dimer resolution sites, because RS^{ET} integrated as efficiently when *dif*1 was located on chromosome 2 as when it was on chromosome 1 (Table 1). Finally, integration was suppressed entirely in *xerC*$^{-}$ cells and did not require homologous recombination (Table S3).

Two Bases Determine the Capacity of RS^{Cl} to Integrate at Both *dif1* and *dif2*. We next investigated which differences in the sequences of RS^{Cl} and RS^{ET} were involved in their different integration behaviors. Because these differences were numerous, we decided to restrict the number of positions tested by searching for CTXϕ residues that would be specifically conserved among classical or El Tor isolates in the available genomic sequences of toxigenic *V. cholerae* strains. During this search, we identified three categories of CTXϕ attachment regions, two of which seemed spe-

Table 1. In vivo integration of RS^{ET} and RS^{Cl}

Phage machinery	*att*P	*dif*	Chromosome	% integration	Screened colonies
Classical	Classical	*dif*1	1	36.4	466
Classical	Classical	*dif*2	2	4.0	451
El Tor	El Tor	*dif*1	1	100.0	454
El Tor	El Tor	*dif*2	2	<0.1	1099
El Tor	Classical	*dif*1	1	100.0	675
El Tor	Classical	*dif*2	2	36.3	1556
Classical	El Tor	*dif*1	1	91.7	743
Classical	El Tor	*dif*2	2	<0.1	883
El Tor	El Tor	*dif*1	2	100.0	875
El Tor	El Tor	*dif*2	1	<0.1	1070

Data were obtained from at least three independent experiments.

cifically linked to classical and El Tor isolates (Fig. 2*A* and Table S4). Indeed, the attachment region of classical variants of CTXϕ, *att*P^{Cl}, differs from the attachment region of El Tor and O139 variants, *att*P^{ET}, by two residues in the overlap region between the XerC- and XerD-binding sites of *att*P2 (Fig. 2*A*, blue residues). Introduction of the classical residues in the attachment region of RS^{ET} led to its efficient integration at both *dif*1 and *dif*2 (Table 1), and introduction of the El Tor residues in the attachment region of RS^{Cl} abolished *dif*2 integration (Table 1), demonstrating that the respective relaxation and specific integration behaviors of RS^{Cl} and RS^{ET} are determined solely by a difference of sequence at these two positions.

XerCD Recombines *att*P^{Cl}(+) with *dif*1 and *dif*2 in Vitro. The T-to-G transversion found in the overlap region of classical *att*P2 allows the recovery of one Watson–Crick bp interaction on one side of the reaction between the (+) ssDNA of *att*P^{Cl} and *dif*2 (Fig. 2*B*, red strand). Perfect Watson–Crick pairing is not recovered on the other side but is replaced by a TG wobble bp (Fig. 2*B*, blue strand). Likewise, one Watson–Crick bp is replaced by a TG wobble bp on one side of the reaction between the stem of the hairpin formed by the (+) ssDNA of *att*P^{Cl} and *dif*1 (Fig. 2*C*, red strand). This finding prompted us to check whether *V. cholerae* XerC and XerD could recombine the (+) ssDNA of *att*P^{Cl} with *dif*1 and *dif*2 in vitro. We did so using purified *V. cholerae* XerC and XerD proteins and annealed synthetic oligonucleotides that mimic *dif*1, *dif*2, and the stems of the hairpins created by *att*P^{Cl} and *att*P^{ET} (Table S5).

Three steps can be defined in the strand exchange reaction performed by tyrosine recombinases: first, a single strand in each of the two recombining sites is cleaved by one recombinase, generating two 3′-phosphorotyrosyl recombinase/DNA covalent intermediates; the liberated 5′-hydroxyl extremities then are exchanged; finally, they attack the phosphorotyrosyl bond of the partner site to form phosphodiester bonds. Cleavage of each of the two recombining strands and their subsequent ligation to the opposite partner strand can be monitored when the strand is labeled at its 3′ extremity: Strand cleavage leads to the apparition of a shorter migration product on a sequencing gel; ligation to a partner strand harboring a longer extension on the 5′ side of the XerC-binding site leads to the creation of a longer recombinant product. Ligation products were detected when *att*P^{ET}(+) was reacted against *dif*1 (Fig. 2*C*, *Upper*) and when *att*P^{Cl}(+) was reacted against *dif*1 or *dif*2 (Fig. 2*D*, *Upper*). Thus, in the absence of any other host or phage factors, XerC and XerD can promote the exchange of one pair of strands when one Watson–Crick bp is replaced by a TG wobble bp on one side of the recombining complex. However, no ligation product was detected between *att*P^{ET}(+) and *dif*2; Watson–Crick pairing is lost on both sides of this reaction (Fig. 2*C*, *Upper*).

Design of a *dif*2-Specific Phage Variant. To demonstrate further that the specificity of integration of the different variants of CTXϕ is governed by the ability to establish bp interactions that stabilize strand exchanges, we designed a phage that, based on the ssDNA integration model, should integrate specifically at *dif*2. To this aim, the thymine immediately downstream of the site of cleavage of XerC was replaced by a cytosine in *att*P^{Cl}(+) [*att*P^{mutCl}(+); Fig. 3*A*]. Because of this substitution, perfect Watson–Crick pairing is lost on both sides of the reaction with *dif*1 (Fig. 3*A*). However, it is re-established on both sides of the reaction with *dif*2 (Fig. 3*A*). As expected, we observed a normal number of XerC-mediated strand exchanges between *att*P^{mutCl}(+) and *dif*2 in vitro, whereas recombination with *dif*1 was barely detectable (Fig. 3*A*). In vivo, this process resulted in the fully specific integration of a vector carrying the *att*P^{mutlCl}(+) attachment site at *dif*2 (*att*P^{mutCl}; Table 2).

Rules of Compatibility Drive the Evolution Between Phage Attachment and Dimer Resolution Sites. We next investigated the sequence of the dimer resolution sites of natural CTXϕ$^-$ *V. cholerae* strains. We found that the first chromosome of many recently isolated O1 El Tor, O139 and non-O1 non-O139 strains harbors a dimer resolution site with an overlap region different from that of *dif*1 and *dif*2; we called this site "*dif*G" (Fig. 3*B* and Table S6). RS^{ET} and RS^{Cl} did not integrate at *dif*G in vivo (Table 2). This result was expected, because no bp interactions could stabilize strand exchanges between *dif*G and *att*P^{ET}(+) or *att*P^{Cl}(+) (Fig. 3*B*). However, the stem of the hairpin created by the folding of the third category of attachment sites that was identified during our database searches (*att*P^{G}; Fig. 2*A*) seemed suitable for integration with *dif*G (Fig. 3*C*). In contrast, *att*P^{G}(+) did not seem suitable for integration at *dif*1 or *dif*2. Correspondingly, *V. cholerae* XerCD specifically recombined *att*P^{G}(+) with *dif*G in vitro (Fig. 3*C*), and a phage harboring *att*P^{G} specifically integrated at *dif*G in vivo (Table 2) independently of the chromosomal context of the site (Table S7).

Discussion

Previous work on the El Tor variant of CTXϕ suggested that it specifically integrates at *dif*1 (6). In this context, the integration of CTXϕ at *dif*2 in classical strains (3) and in recent El Tor isolates (4, 10–14) was puzzling. It was observed recently that El Tor strains can acquire the *dif*2-integrated classical copy of CTXϕ via chitin-induced competence and homologous recombination (18). However, such a mechanism left open the questions of how *dif*2 integration could be achieved initially and the frequency at which this integration could occur. In addition, it did not explain the diversity of combinations of the different genetic elements that were found integrated at the chromosome dimer resolution sites loci of *V. cholerae* strains (4). To address these points, we designed a sensitive assay to monitor the spe-

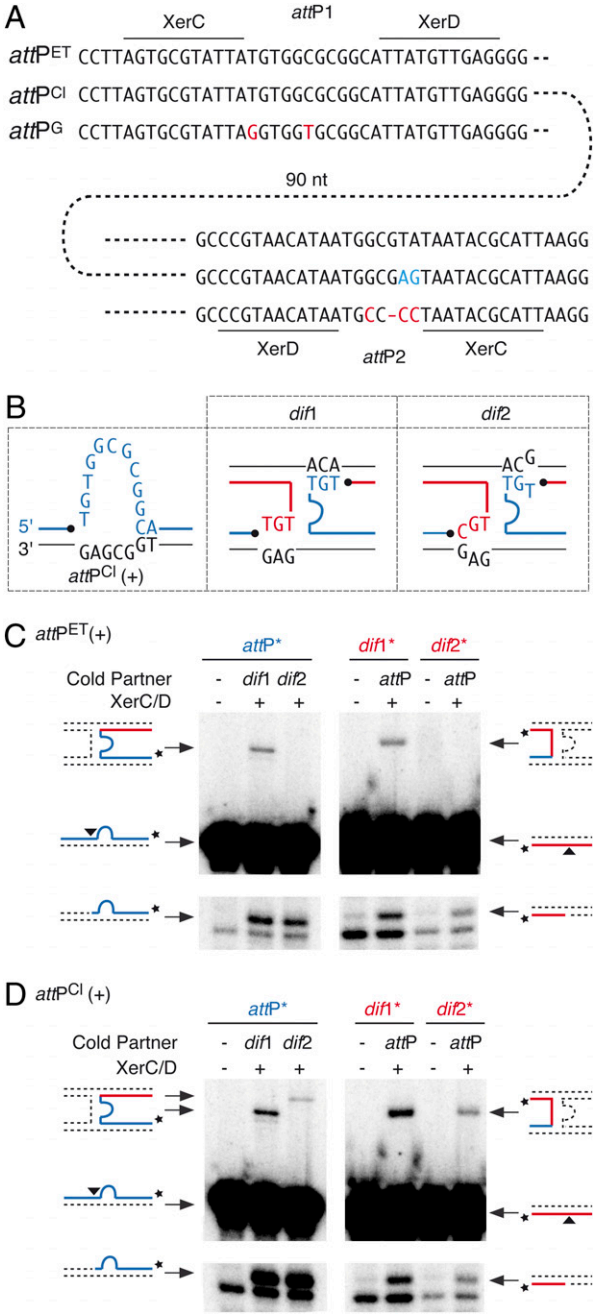

Fig. 2. The (+) ssDNA of classical variants of CTXϕ recombines with both *dif*1 and *dif*2. (*A*) The three categories of phage attachment regions found in CTXϕ variants. Residues specifically conserved in classical and G variants of the phage are shown in blue and red, respectively. (*B*) Schemes of Watson–Crick bp interactions that could stabilize the strand exchange catalyzed by XerC between the overlap regions of the two dimer resolution sites of N16961 and the attachment site found in the (+) ssDNA genome of classical variants of CTXϕ. The legend is as in Fig. 1*C*. (*C*) *V. cholerae* XerCD-mediated recombination of *att*P^{ET}(+) with *dif*1 and *dif*2. A short radioactively labeled *att*P substrate was reacted with a longer cold dimer resolution substrate (*Left Panels*), and a short radioactively labeled dimer resolution substrate was reacted with a longer cold *att*P substrate (*Right Panels*). Schemes of substrate and products are indicated on the side of each panel. A black triangle indicates the position of cleavage of *V. cholerae* XerC. A star indicates the position of the radioactive label of the probe. (*D*) *V. cholerae* XerCD-mediated recombination of *att*P^{CI}(+) with *dif*1 and *dif*2. Schemes of the products and of the substrate are indicated as in Fig. 2*B*.

cificity and efficiency of *dif*1 and *dif*2 integration events. We then cloned the replication and integration region of the variant of CTXϕ found in the 569B classical strain into a vector harboring a conditional origin of replication; this vector was delivered into N16961 El Tor cells by conjugation. Surprisingly, we observed that this vector efficiently integrated at both *dif*1 and *dif*2 independently of the chromosomal context of the sites (Table 1). This result explains how the classical variant of CTXϕ could integrate in the genome of classical strains even if their two chromosomes share the same *dif*2 dimer resolution site (CP000626.1) and why it was found integrated at *dif*1 on the first chromosome of the El Tor BX330286 strain although such a configuration had not been observed previously in any other strain (4). In contrast, the N16961 El Tor variant of CTXϕ specifically targeted *dif*1 (Table 1). Likewise, we observed that classical and El Tor variants of CTXϕ could not integrate at *dif*G, the dimer resolution site on the larger chromosome of many nontoxigenic strains, but that *dif*G is targeted specifically by a third type of phage that was isolated recently (Table 2).

CTXϕ integration is irreversible (6, 9), and the secretion of new phage particles relies on the production of its ssDNA genome by rolling circle replication across tandemly integrated copies (20, 21). However, we observed that RS^{CI} can integrate in tandem copies that should ensure such a production (Fig. S1). Correspondingly, the sequencing of the genome of several *V. cholerae* strains revealed the presence of tandem copies of the classical phage (El Tor strains BX330286 and B33) (4). In addition, it was observed that classical copies of the phage coexist with intact El Tor copies and/or with the RS1 element in other strains (4, 14); such coexistence also could ensure the production of classical CTXϕ virions. Interestingly, the conjunct production of El Tor and classical phages could favor the emergence of hybrid phages, a phenomenon that has been observed recently (Fig. 1*A*) (4, 13). Taken together, these observations suggest that lysogenic conversion by CTXϕ is the primary mode of acquisition of the cholera toxin genes; this mode of acquisition, along with the evolution of phage attachment and chromosome dimer resolution sites, contributes to the generation of genetic diversity among cholera epidemic strains.

Our results further indicate that the relaxation and specific integration behaviors of the classical and the El Tor variants of CTXϕ are determined solely by a difference in sequence at two positions in the seven-bp overlap region of *att*P2, immediately 3′ to the position at which XerC should cleave (Fig. 1*B*). Two models have been proposed for CTXϕ integration at *dif*1 (8, 9). In the first model, XerCD would catalyze the formation of a Holliday junction between the host dimer resolution sites and the dsDNA form of *att*P1, which is found on the replicative form of the phage (8). In this model, *att*P2 is thought to play a structural role in stabilizing the synapse and/or the exchange; this assumption makes it difficult to explain how mutations in its overlap region could influence the specificity of integration. In contrast, the base immediately 3′ to the XerC cleavage site in the overlap region of *att*P2 contributes to the formation of bp interactions during the strand exchange predicted by the ssDNA integration model (Fig. 1*C*) (9). Here, we show that all of the combinations between (+) ssDNA phage attachment sites and chromosome dimer resolution sites in which Watson–Crick bp interactions could stabilize the exchange of strands catalyzed by XerC [*att*P^{ET}(+)x*dif*1, *att*P^{mutCl}(+)x*dif*2, and *att*P^{G}(+)x*dif*G] were recombined in vitro and promoted integration in vivo. No in vitro recombination and no in vivo integration were detected for combinations in which no Watson–Crick bp interactions could be formed [*att*P^{ET}(+)x*dif*2, *att*P^{mutCl}(+)x*dif*1, *att*P^{G}(+)x*dif*1, and *att*P^{G}(+)x*dif*2]. In the remaining two combinations we tested [*att*P^{Cl}(+)x*dif*1 and *att*P^{Cl}(+)x*dif*2], proper Watson–Crick bps could form only on one side of the recombi-

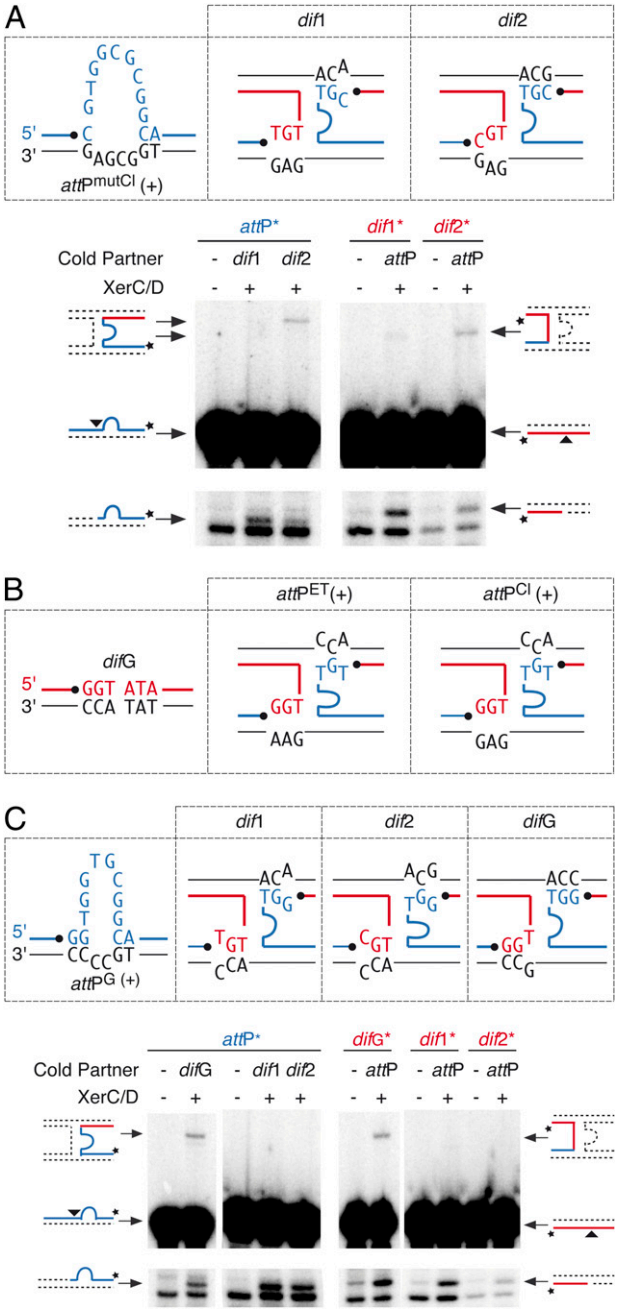

Fig. 3. Homology determinants implicated in lysogenic conversion. (*A*) Design of a variant of CTXϕ specifically integrating at *dif*2. The legend is as in Figs. 1*C* and 2*C*. (*B*) Scheme showing the possible pairing interactions between *difG* and *attP*^{ET}(+) or *attP*^{Cl}(+). The legend is as in Fig. 1*C*. (*C*) *V. cholerae* XerCD-mediated recombination of *attP*^{G}(+) with *dif*1, *dif*2, and *difG*. A scheme of the possible pairing interactions is shown above the gels. The legend is as in Figs. 1*C* and 2*C*.

nation complex, but nevertheless in vitro recombination and in vivo integration were observed. To stabilize the exchange of strands, tyrosine recombinases normally require one Watson–Crick bp interaction on each side of the recombination complex immediately after the position of cleavage of the recombinases (22–31). The only notable exception to this rule is the integrase of some bacteroides conjugative transposons (32). In this context, it does not seem fortuitous that a TG wobble bp replaces the missing Watson–Crick bp in reactions between *attP*^{Cl}(+) and *dif*1 or *dif*2 (Fig. 2*B*). Taken together, these results give considerable support to the ssDNA integration model and allow the definition of rules of compatibility between phage attachment and dimer resolution sites that dictate the possibility for lysogenic conversion.

Table 2. Integration compatibility of CTXϕ *attP*(+) sites and of *dif* sites

Phage machinery	*attP*	*dif*	% integration	Screened colonies
El Tor	mutCl	*dif*1*	<0.1	1256
El Tor	mutCl	*dif*2*†	30.4	1449
El Tor	El Tor	*difG**	<0.1	1335
Classical	Classical	*difG**	<0.1	1399
El Tor	G	*difG**	1.1	2110
El Tor	G	*dif*1*	<0.3	307
El Tor	G	*dif*2*†	<0.4	271

Data were obtained from at least three independent experiments.
*On chromosome 1.
†On chromosome 2.

Finally, in four of the five effective combinations of attachment and dimer resolution sites we tested [*attP*^{ET}(+)x*dif*1, *attP*^{Cl}(+)x*dif*1, *attP*^{Cl}(+)x*dif*2, and *attP*^{mutCl}(+)x*dif*2], the efficiency of integration correlated with the efficiency of recombination observed in vitro. Furthermore, the in vitro recombination efficiency of these four combinations (Fig. 2 *C* and *D* and Fig. 3*A*, *Upper*) correlated with the stability and/or frequency of formation of the two cleaved substrates involved in the strand exchange (Fig. 2 *C* and *D* and Fig. 3*A*, *Lower*). For instance, the lower efficiency of the recombination of *attP*^{mutCl}(+)x*dif*2 when compared with *attP*^{ET}(+)x*dif*1, *attP*^{Cl}(+)x*dif*1, and *attP*^{Cl}(+)x*dif*2 is explained by the lower stability of the *dif*2/XerC and *attP*^{mutCl}/XerC covalent complexes compared with the *dif*1/XerC, *attP*^{ET}/XerC, and *attP*^{Cl}/XerC covalent complexes (with respective mean frequencies of 0.15 ± 0.08%, 0.16 ± 0.08%, 0.46 ± 0.18%, 0.41 ± 0.12%, and 1.19 ± 0.65% out of at least four independent experiments). The relatively low number of *dif*2/XerC covalent intermediates fits with previous results that indicated that the control of recombination is more stringent at *dif*2 than at *dif*1 (5). The relatively low number of *attP*^{mutCl}/XerC covalent intermediates further suggests that the presence of a cytosine immediately 5′ to the XerC cleavage site is detrimental to XerC cleavage and/or to the stability of the cleaved complex. In contrast, the frequency with which a vector carrying the *attP*^{G} attachment region integrated at *difG* was low when compared with the efficiency of the *attP*^{G}(+)x*difG* recombination reaction in vitro (Table 2 and Fig. 3*B*). This finding suggests that factors other than the efficiency with which strand exchanges are performed govern CTXϕ lysogeny. Such factors also could explain why integration was less efficient for vectors harboring the classical replication machinery than for vectors harboring the El Tor replication machinery (Tables 1 and 2). Some factors could play a role in the production and/or stabilization of the (+) ssDNA genome of the phage. Others might play a role in the conversion of the Holliday junction intermediate into fully recombinant products by repair and/or replication. The observation that *attP*^{G} and RS^{Cl} are detrimental to some of these factors should help unravel these other important aspects of CTXϕ integration.

Methods

Strains and Plasmids. Relevant strains and plasmids are described in Tables S1 and S2, respectively. Both *E. coli* and *V. cholerae* cells were grown in LB at 37 °C with shaking (220 rpm). Unless otherwise indicated, cognate antibiotics were used at the following concentrations: streptomycin, 100 μg/mL; spectinomycin, 100 μg/mL; chloramphenicol, 34 μg/mL for *E. coli* and 3 μg/mL for *V. cholerae*; and rifampicin, 100 μg/mL for *E. coli* and 2 μg/mL for *V. cholerae*. All *V. cholerae* reporter strains were constructed by allele exchange methods

using derivatives of suicide vectors carrying either *sacB* or *rpsL* as a counter selectable marker (33, 34). Engineered strains were confirmed by PCR and sequencing. For long storage, cells were maintained at −70 °C in LB containing 20% glycerol. Classical and El Tor phage replication and integration machinery (RS elements) were amplified using genomic DNA of *V. cholerae* strains 569B or N16961, respectively, as templates. The amplicons were cloned into the suicide vector pSW23T (30). Plasmids carrying hybrid phage variants were engineered by inverse PCR. The recombinant suicide vectors carrying the functional *lacZ*::*dif* allele flanking by the chromosomal fragments of *V. cholerae* were constructed by cloning the 28-bp *dif* site in the natural ClaI site of the *E. coli lacZ* gene.

In Vivo Integration Assay. For conjugation both donor [diaminopimelic acid (DAP) auxotroph *E. coli*)] and recipient (*V. cholerae*) strains were grown separately in LB to an OD of ∼0.3 at 600 nm. Bacteria were pelleted by centrifugation, washed, and mixed in 25% of the initial volume in fresh LB supplemented with 0.3 mM DAP. The mixture then was deposited on a sterile filter paper covering an LB-agar plate supplemented with DAP. After 4 h of incubation at 37 °C, bacterial cells were resuspended and plated on LB plates containing X-gal isopropyl β-D-1-thiogalactopyranoside (IPTG) and cognate antibiotics. Transconjugants carrying integrated or replicative forms of phage machinery were monitored after 36 h of growth at 37 °C.

Protein Purification. The XerC and XerD ORFs were amplified by PCR from N16961 genome and cloned into the pTYB-11 (New England Biolabs) expression vector using SapI and PstI restriction sites. Proteins were produced at 30 °C in BL21Gold cells (Stratagene). XerD-producing cells were grown for 2 h in the presence of 0.1 mM IPTG. XerC-producing cells were grown for 2 h in the presence of 0.2% glucose and 0.5 mM IPTG. Cells were collected and resuspended in buffer A (25 mM TrisHCl, pH8/1 M NaCl/10% glycerol), frozen in dry ice, and lysed with a Carver press. Lysates were centrifuged for 1 h at 25,000 × *g*. The supernatants were loaded on chitin bead columns and washed extensively with buffer A. Intein tag cleavage was performed in buffer A adjusted to 0.5 M NaCl and supplemented with 50 mM DTT at 7 °C for 16 h. Untagged XerC and XerD were eluted, and small aliquots were frozen and stored at −70 °C. Protein concentrations were evaluated by the Bradford methods using BSA as standard.

In Vitro Recombination Assays. Synthetic oligos used to mimic *dif*1, *dif*2, *dif*G, *att*P^{ET}, *att*P^{CI}, *att*P^{mutCI}, and *att*P^{G} are shown in Table S5. Recombination reactions were performed in a 20-μL volume, in the presence of 25 mM Tris-HCl (pH 7.4), 100 mM NaCl, 1 mM EDTA, 0.1 μg/mL BSA, 40% glycerol, and 5 nM each of the cold and radioactively labeled recombination substrates. XerC and XerD were used at 150 nM and 100 nM final concentrations, respectively. Reactions were incubated for 3 h at 37 °C, ethanol precipitated, and analyzed by PAGE using a 10% acrylamide-urea gel. Dried gels were exposed to phosphor screen. Signals were detected using a Typhoon instrument and quantitated using the IQT 7.0 software (GE Healthcare).

ACKNOWLEDGMENTS. We thank R.K. Bhadra and D. Mazel for the kind gift of *V. cholerae* strains and C. Possoz for helpful discussions. This work was supported by the Fondation pour la Recherche Médicale (Equipe 2007), the European Molecular Biology Organization (YIP 2006), and the Centre National pour la Recherche Scientifique (ATIP+).

1. De SN (1959) Enterotoxicity of bacteria-free culture-filtrate of *Vibrio cholerae*. *Nature* 183:1533–1534.
2. Waldor MK, Mekalanos JJ (1996) Lysogenic conversion by a filamentous phage encoding cholera toxin. *Science* 272:1910–1914.
3. Davis BM, Moyer KE, Boyd EF, Waldor MK (2000) CTX prophages in classical biotype *Vibrio cholerae*: Functional phage genes but dysfunctional phage genomes. *J Bacteriol* 182:6992–6998.
4. Chun J, et al. (2009) Comparative genomics reveals mechanism for short-term and long-term clonal transitions in pandemic *Vibrio cholerae*. *Proc Natl Acad Sci USA* 106: 15442–15447.
5. Val M-E, et al. (2008) FtsK-dependent dimer resolution on multiple chromosomes in the pathogen *Vibrio cholerae*. *PLoS Genet* 4:e1000201.
6. Huber KE, Waldor MK (2002) Filamentous phage integration requires the host recombinases XerC and XerD. *Nature* 417:656–659.
7. Barre F-X, Sherratt DJS (2002) Xer site-specific recombination: Promoting chromosome segregation. *Mobile DNA II*, eds Craig NL, Craigie R, Gellert M, Lambowitz A (ASM Press, Washington, D.C.), Vol 1, pp 149–161.
8. McLeod SM, Waldor MK (2004) Characterization of XerC- and XerD-dependent CTX phage integration in *Vibrio cholerae*. *Mol Microbiol* 54:935–947.
9. Val M-E, et al. (2005) The single-stranded genome of phage CTX is the form used for integration into the genome of *Vibrio cholerae*. *Mol Cell* 19:559–566.
10. Das B, Halder K, Pal P, Bhadra RK (2007) Small chromosomal integration site of classical CTX prophage in Mozambique *Vibrio cholerae* O1 biotype El Tor strain. *Arch Microbiol* 188:677–683.
11. Faruque SM, et al. (2007) Genomic analysis of the Mozambique strain of *Vibrio cholerae* O1 reveals the origin of El Tor strains carrying classical CTX prophage. *Proc Natl Acad Sci USA* 104:5151–5156.
12. Ledón T, et al. (2008) El Tor and Calcutta CTXPhi precursors coexisting with intact CTXPhi copies in *Vibrio cholerae* O139 isolates. *Res Microbiol* 159:81–87.
13. Minh NB, et al. (2009) Cholera outbreaks caused by an altered *Vibrio cholerae* O1 El Tor biotype strain producing classical type cholera toxin B in Vietnam 2007-2008. *J Clin Microbiol* .
14. Raychoudhuri A, et al. (2009) Classical ctxB in *Vibrio cholerae* O1, Kolkata, India. *Emerg Infect Dis* 15:131–132.
15. Hung DT, Mekalanos JJ (2005) Bile acids induce cholera toxin expression in *Vibrio cholerae* in a ToxT-independent manner. *Proc Natl Acad Sci USA* 102:3028–3033.
16. Mekalanos JJ (1983) Duplication and amplification of toxin genes in *Vibrio cholerae*. *Cell* 35:253–263.
17. Kaper JB, Morris JG, Jr, Levine MM (1995) Cholera. *Clin Microbiol Rev* 8:48–86.
18. Udden SM, et al. (2008) Acquisition of classical CTX prophage from *Vibrio cholerae* O141 by El Tor strains aided by lytic phages and chitin-induced competence. *Proc Natl Acad Sci USA* 105:11951–11956.
19. Waldor MK, Rubin EJ, Pearson GD, Kimsey H, Mekalanos JJ (1997) Regulation, replication, and integration functions of the *Vibrio cholerae* CTXphi are encoded by region RS2. *Mol Microbiol* 24:917–926.
20. Davis BM, Waldor MK (2000) CTXphi contains a hybrid genome derived from tandemly integrated elements. *Proc Natl Acad Sci USA* 97:8572–8577.
21. Moyer KE, Kimsey HH, Waldor MK (2001) Evidence for a rolling-circle mechanism of phage DNA synthesis from both replicative and integrated forms of CTXphi. *Mol Microbiol* 41:311–323.
22. Arciszewska L, Grainge I, Sherratt D (1995) Effects of Holliday junction position on Xer-mediated recombination in vitro. *EMBO J* 14:2651–2660.
23. Nunes-Düby SE, Yu D, Landy A (1997) Sensing homology at the strand-swapping step in lambda excisive recombination. *J Mol Biol* 272:493–508.
24. Nunes-Düby SE, Azaro MA, Landy A (1995) Swapping DNA strands and sensing homology without branch migration in lambda site-specific recombination. *Curr Biol* 5:139–148.
25. Lee SY, Landy A (2004) The efficiency of mispaired ligations by lambda integrase is extremely sensitive to context. *J Mol Biol* 342:1647–1658.
26. Zhu XD, Pan G, Luetke K, Sadowski PD (1995) Homology requirements for ligation and strand exchange by the FLP recombinase. *J Biol Chem* 270:11646–11653.
27. Lee J, Jayaram M (1995) Role of partner homology in DNA recombination. Complementary base pairing orients the 5′-hydroxyl for strand joining during Flp site-specific recombination. *J Biol Chem* 270:4042–4052.
28. Hoess RH, Wierzbicki A, Abremski K (1986) The role of the loxP spacer region in P1 site-specific recombination. *Nucleic Acids Res* 14:2287–2300.
29. MacDonald D, Demarre G, Bouvier M, Mazel D, Gopaul DN (2006) Structural basis for broad DNA-specificity in integron recombination. *Nature* 440:1157–1162.
30. Demarre G, et al. (2005) A new family of mobilizable suicide plasmids based on broad host range R388 plasmid (IncW) and RP4 plasmid (IncPalpha) conjugative machineries and their cognate *Escherichia coli* host strains. *Res Microbiol* 156:245–255.
31. Barabas O, et al. (2008) Mechanism of IS200/IS605 family DNA transposases: Activation and transposon-directed target site selection. *Cell* 132:208–220.
32. Malanowska K, Yoneji S, Salyers AA, Gardner JF (2007) CTnDOT integrase performs ordered homology-dependent and homology-independent strand exchanges. *Nucleic Acids Res* 35:5861–5873.
33. Philippe N, Alcaraz JP, Coursange E, Geiselmann J, Schneider D (2004) Improvement of pCVD442, a suicide plasmid for gene allele exchange in bacteria. *Plasmid* 51: 246–255.
34. Skorupski K, Taylor RK (1996) Positive selection vectors for allelic exchange. *Gene* 169: 47–52.

Supporting Information

Das et al. 10.1073/pnas.0910212107

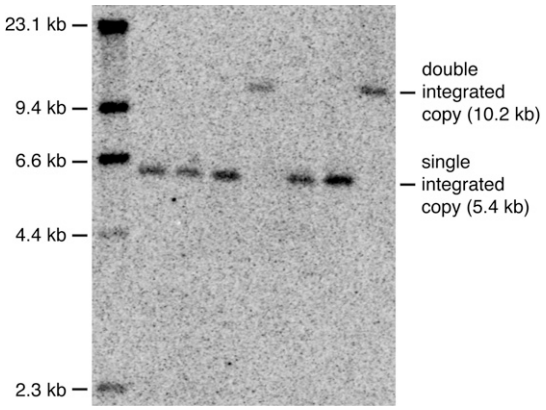

Fig. S1. Tandem integration of the classical variant of CTXϕ. The genomic DNA from BS1 bacteria in which RS^{CI} had integrated successfully was subjected to Hpa1 restriction digest. Restriction fragments were separated by agarose gel electrophoresis and blotted on a PVDF membrane. The *dif*1-containing fragment was revealed by hybridization with a radioactive probe made from the Hpa1 lacZ fragment.

Table S1. Strain list.

Strains	Genotype/phenotypes	References/resources
N16961	O1 El Tor strain, St^r	(1)
569B	O1 classical strain, St^r	D. Mazel Lab., Pasteur
H12	CTXϕ- O1 El Tor strain	RK Bhadra Lab., IICB
H25	CTXϕ- O1 El Tor strain	RK Bhadra Lab., IICB
WO-5	CTXϕ- O1 El Tor strain	RK Bhadra Lab., IICB
MV18	N16961 Δ*lacZ* Δ(RS2 RS1 *dif*1)::*aadA1*; Sp^r St^r	This study
MV78	MV18 $lacZ_{Ec}$::*dif1*; St^r	This study
BS1	MV78 Δ*dif2*::*aadA1*; Sp^r St^r	This study
BS2	MV18 Δ*dif2*::*arr2*; Sp^r St^r Rf^r	This study
BS3	BS2 in which Δ*dif2*::*arr2* was replaced by $lacZ_{Ec}$::*dif2*	This study
BS10	BS1 Δ*xerC*::*arr2*; Sp^r St^r Rf^r	This study
BS11	BS1 Δ*recA*; Sp^r St^r	This study
BS12	BS2 in which Δ*dif2*::*arr2* was replaced by $lacZ_{Ec}$::*dif1*	This study
BS13	BS2 in which Δ*dif1*::*aadA1* was replaced by $lacZ_{Ec}$::*dif2*	This study
BS14	BS2 in which Δ*dif1*::*aadA1* was replaced by $lacZ_{Ec}$::*difG*	This study
BS15	BS2 in which Δ*dif2*::*arr2* was replaced by $lacZ_{Ec}$::*difG*	This study

1. Heidelberg JF, et al. (2000) DNA sequence of both chromosomes of the cholera pathogen *Vibrio cholerae*. *Nature* 406:477–483.

Table S2. Plasmid list.

Name	Description	References/resources
pSW23T	pSW23::oriTRP4; oriVR6Kγ; Cm^r	(1)
pDS132	pCVD442 derivative carrying the *sac*B counter selectable marker; Cm^r	(2)
pKAS32	pGP704 derivative carrying the *rps*L counter selectable marker; Ap^r	(3)
pBS22	RS$_{Cl}$; pSW23T harboring the replication and integration machinery of the CTXϕ prophage of *V. cholerae* strain 569B; Cm^r	This study
pBS39	pBS22 where *att*P^{Cl} was modified into *att*P^{ET}; Cm^r	This study
pMEV30	RS$_{ET}$; pSW23T harboring the replication and integration machinery of RS1, a CTXϕ satellite phage of *V. cholerae strain* N16961; Cm^r	This study
pBS4	pMEV30 in which *att*P^{ET} was modified into *att*P^{Cl}; Cm^r	This study
pBS15	pBS4 in which *att*P^{Cl} was modified into *att*P^{mutCl}; Cm^r	This study
pBS35	pMEV30 in which *att*P^{ET} was modified into *att*P^{G}; Cm^r	This study
pMEV136	pDS132 carrying an *aad*1 cassette flanked by the upstream and downstream regions of *dif*1; Cm^r, Sp^r	This study
pBS8	pKAS32 carrying an *aad*1 cassette flanked by the upstream and downstream regions of *dif*2; Ap^r, Sp^r	This study
pMEV235	pDS132 carrying an *arr*2 cassette flanked by the upstream and downstream regions of *dif*2; Cm^r, Rf^r	This study
pMEV78	pDS132 carrying the *lac*Z::*dif*1 allele flanked by the upstream and downstream regions of *dif*1; Cm^r	This study
pBS3	pDS132 carrying the *lac*Z::*dif*2 allele flanked by the upstream and downstream regions of *dif*2; Cm^r	This study
pBS24	pDS132 carrying the *lac*Z::*dif*2 allele flanked by the upstream and downstream regions of *dif*1; Cm^r	This study
pMEV184	pDS132 carrying the *lac*Z::*dif*1 allele flanked by the upstream and downstream regions of *dif*2; Cm^r	This study
pBS42	pDS132 carrying the *lac*Z::*dif*G allele flanked by the upstream and downstream regions of *dif*1; Cm^r	This study
pBS38	pDS132 carrying the *lac*Z::*dif*G allele flanked by the upstream and downstream regions of *dif*2; Cm^r	This study
pMEV245	pDS132 carrying an *arr*2 cassette flanked by the upstream and downstream region of *V. cholerae* *xer*C; Cm^r, Rf^r	This study
pMEV68	pDS132 carrying the upstream and downstream regions of *V. cholerae* *rec*A; Cm^r	(4)

1. Demarre G, et al. (2005) A new family of mobilizable suicide plasmids based on broad host range R388 plasmid (IncW) and RP4 plasmid (IncPalpha) conjugative machineries and their cognate *Escherichia coli* host strains. *Res Microbiol* 156:245–255.
2. Philippe N, Alcaraz JP, Coursange E, Geiselmann J, Schneider D (2004) Improvement of pCVD442, a suicide plasmid for gene allele exchange in bacteria. *Plasmid* 51:246–255.
3. Skorupski K, Taylor RK (1996) Positive selection vectors for allelic exchange. *Gene* 169:47–52.
4. Val M-E, et al. (2008) FtsK-dependent dimer resolution on multiple chromosomes in the pathogen Vibrio cholerae. *PLoS Genet* 4:e1000201.

Table S3. *dif*1 integration of CTXϕ in *recA*$^-$ and *xerC*$^-$ strains

Phage machinery	*att*P sequence	Host machinery	% Integration	Screened colonies
El Tor	El Tor	*recA*$^-$	100.0	180
El Tor	El Tor	*xerC*$^-$	<0.5	183
Classical	Classical	*recA*$^-$	47.4	76
Classical	Classical	*xerC*$^-$	<0.2	550

Table S4. The category of the *att*P attachment region of various CTXϕ variants

Phage origin	*att*P category
VC44RS1J2E	El Tor
AB299799	El Tor
VC44RS1J1E	El Tor
N16961	El Tor
O139AY101180	El Tor
VCU83796	El Tor
AF510994	Classical
AF175708	Classical
AY349175	Classical
DQ012295	Classical
O395LRS2C	Classical
O395SRS2C	Classical
AF110029	Classical
AF238372	Classical
AF30279	G
AF416590	G

Table S5. Oligonucleotides used in this study

Name	Sequence
Dif1top	5′ATCAGTGCGCATTATGTATGTTATGTTAAATGGA
Dif1bot	5′CTGTCCATTTAACATAACATACATAATGCGCACTGAT
Dif2top	5′ATCAATGCGCATTACGTGCGTTATGTTAAATGGA
Dif2bot	5′CTGTCCATTTAACATAACGCACGTAATGCGCATTGAT
DifGtop	5′ATCAGTGCGCATTAGGTATATTATGTTAAATGGA
DifGbot	5′CTGTCCATTTAACATAATATACCTAATGCGCACTGAT
AttPdif1top	5′TACGCCCTTAGTGCGTATTATGTGGCGCGGCATTATGTTGAGGGTTCCG
AttPdif1bot	5′CTGCGGAACCCGTAACATAATGGCGTATAATACGCATTAAGGGCGTA
AttPmutClbot	5′CTGCGGAACCCGTAACATAATGGCGAGTAATACGCATTAAGGGCGTA
AttPmuCltop	5′TACGCCCTTAGTGCGTATTACGTGGCGCGGCATTATGTTGAGGGTTCCG
AttPGtop	5′TACGCCCTTAGTGCGTATTAGGTGGTGCGGCATTATGTTGAGGGTTCCG
AttPGbot	5′CTGCGGAACCCGTAACATAATGCCCCTAATACGCATTAAGGGCGTA
Dif2topextended	5′TAATCTAGATTATGCCTTAATTTAACATAACGCACGTAATGCGCATTAAGTGTTCGTAGGTCGACGAT
Dif2botextended	5′ATCGTCGACCTACGAACACTTAATGCGCATTACGTGCGTTATGTTAAATTAAGGCATAATCTAGATTA
DifGtopextended	5′CAATCTAGACCGCCGCCTTAGTGCGCATTAGGTATATTATGTTAAATTAAGGCATAATGTCGACAA
DifGbotextended	5′TTGTCGACATTATGCCTTAATTTAACATAATATACCTAATGCGCACTAAGGCGGCGGTCTAGATTG
Dif1topextended	5′CAATCTAGACCGCCGCCTTAGTGCGCATTATGTATGTTATGTTAAATTAAGGCATAATGTCGACAA
Dif1botextended	5′TTGTCGACATTATGCCTTAATTTAACATAACATACATAATGCGCACTAAGGCGGCGGTCTAGATTG

Table S6. Sequence of *dif*1 in different CTXϕ-negative strains

Strain	Serotype	*dif*1 sequence	CTX	Sources
N16961	O1 (ET)	AGTGCGTATTA TGTATG TTATGTTAAAT	+	(1)
O395	O1 (Cl)	AATGCGTATTA CGTGCG TTATGTTAAAT	+	CP000626.1
H25	O1 (ET)	AGTGCGTATTA GGTATA TTATGTTAAAT	–	This study
H12	O1 (ET)	AGTGCGTATTA GGTATA TTATGTTAAAT	–	This study
WO5	O1 (ET)	AGTGCGTATTA GGTATA TTATGTTAAAT	–	This study
Ku-40	O1 (ET)	AGTGCGTATTA GGTATA TTATGTTAAAT	–	AY368493.1
93333	O139	AGTGCGTATTA GGTATA TTATGTTAAAT	–	AY368494.1
AM19226	Non O1/ non O139	AGTGCGTATTA GGTATA TTATGTTAAAA	–	(2)
1587	Non O1/ non O139	AGTGCGTATTA GGTATA TTATGTTAAAT	–	(2)
RC385	Non O1/ non O139	AGTGCGTATTA GGTGTA TTATGTTAAAA	–	(2)

1. Val M-E, et al. (2008) FtsK-dependent dimer resolution on multiple chromosomes in the pathogen *Vibrio cholerae*. *PLoS Genet* 4:e1000201.
2. Faruque SM, et al. (2007) Genomic analysis of the Mozambique strain of *Vibrio cholerae* O1 reveals the origin of El Tor strains carrying classical CTX prophage. *Proc Natl Acad Sci USA* 104:5151–5156.

Table S7. *dif*G integration of CTXϕ on the second chromosome of V. *cholerae*

Phage machinery	*att*P sequence	*dif* sequence	% integration	Number of screened colonies
El Tor	El Tor	*dif*G	<0.2	625
Classic	Classic	*dif*G	<0.1	1526
El Tor	G	*dif*G	2.2	1598

Supporting Information

Das et al. 10.1073/pnas.0910212107

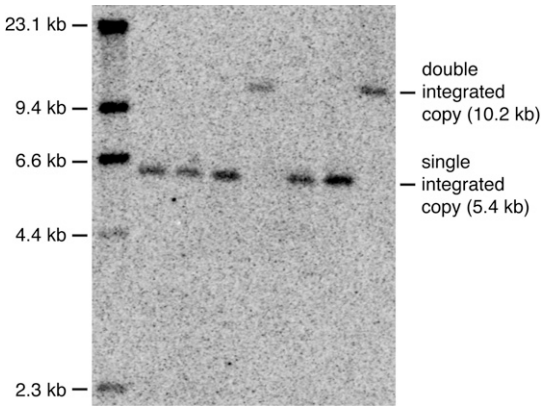

Fig. S1. Tandem integration of the classical variant of CTXϕ. The genomic DNA from BS1 bacteria in which RS^{CI} had integrated successfully was subjected to Hpa1 restriction digest. Restriction fragments were separated by agarose gel electrophoresis and blotted on a PVDF membrane. The *dif*1-containing fragment was revealed by hybridization with a radioactive probe made from the Hpa1 lacZ fragment.

Table S1. Strain list.

Strains	Genotype/phenotypes	References/resources
N16961	O1 El Tor strain, St^r	(1)
569B	O1 classical strain, St^r	D. Mazel Lab., Pasteur
H12	CTXϕ- O1 El Tor strain	RK Bhadra Lab., IICB
H25	CTXϕ- O1 El Tor strain	RK Bhadra Lab., IICB
WO-5	CTXϕ- O1 El Tor strain	RK Bhadra Lab., IICB
MV18	N16961 Δ*lacZ* Δ(RS2 RS1 *dif*1)::*aadA1*; Sp^r St^r	This study
MV78	MV18 $lacZ_{Ec}$::*dif1*; St^r	This study
BS1	MV78 Δ*dif2*::*aadA1*; Sp^r St^r	This study
BS2	MV18 Δ*dif2*::*arr2*; Sp^r St^r Rf^r	This study
BS3	BS2 in which Δ*dif2*::*arr2* was replaced by $lacZ_{Ec}$::*dif2*	This study
BS10	BS1 Δ*xerC*::*arr2*; Sp^r St^r Rf^r	This study
BS11	BS1 Δ*recA*; Sp^r St^r	This study
BS12	BS2 in which Δ*dif2*::*arr2* was replaced by $lacZ_{Ec}$::*dif1*	This study
BS13	BS2 in which Δ*dif1*::*aadA1* was replaced by $lacZ_{Ec}$::*dif2*	This study
BS14	BS2 in which Δ*dif1*::*aadA1* was replaced by $lacZ_{Ec}$::*difG*	This study
BS15	BS2 in which Δ*dif2*::*arr2* was replaced by $lacZ_{Ec}$::*difG*	This study

1. Heidelberg JF, et al. (2000) DNA sequence of both chromosomes of the cholera pathogen *Vibrio cholerae*. *Nature* 406:477–483.

Table S2. Plasmid list.

Name	Description	References/resources
pSW23T	pSW23::oriTRP4; oriVR6Kγ; Cm^r	(1)
pDS132	pCVD442 derivative carrying the *sac*B counter selectable marker; Cm^r	(2)
pKAS32	pGP704 derivative carrying the *rps*L counter selectable marker; Ap^r	(3)
pBS22	RS$_{Cl}$; pSW23T harboring the replication and integration machinery of the CTXϕ prophage of *V. cholerae* strain 569B; Cm^r	This study
pBS39	pBS22 where *att*P^{Cl} was modified into *att*P^{ET}; Cm^r	This study
pMEV30	RS$_{ET}$; pSW23T harboring the replication and integration machinery of RS1, a CTXϕ satellite phage of *V. cholerae strain* N16961; Cm^r	This study
pBS4	pMEV30 in which *att*P^{ET} was modified into *att*P^{Cl}; Cm^r	This study
pBS15	pBS4 in which *att*P^{Cl} was modified into *att*P^{mutCl}; Cm^r	This study
pBS35	pMEV30 in which *att*P^{ET} was modified into *att*P^{G}; Cm^r	This study
pMEV136	pDS132 carrying an *aad*1 cassette flanked by the upstream and downstream regions of *dif*1; Cm^r, Sp^r	This study
pBS8	pKAS32 carrying an *aad*1 cassette flanked by the upstream and downstream regions of *dif*2; Ap^r, Sp^r	This study
pMEV235	pDS132 carrying an *arr*2 cassette flanked by the upstream and downstream regions of *dif*2; Cm^r, Rf^r	This study
pMEV78	pDS132 carrying the *lac*Z::*dif*1 allele flanked by the upstream and downstream regions of *dif*1; Cm^r	This study
pBS3	pDS132 carrying the *lac*Z::*dif*2 allele flanked by the upstream and downstream regions of *dif*2; Cm^r	This study
pBS24	pDS132 carrying the *lac*Z::*dif*2 allele flanked by the upstream and downstream regions of *dif*1; Cm^r	This study
pMEV184	pDS132 carrying the *lac*Z::*dif*1 allele flanked by the upstream and downstream regions of *dif*2; Cm^r	This study
pBS42	pDS132 carrying the *lac*Z::*dif*G allele flanked by the upstream and downstream regions of *dif*1; Cm^r	This study
pBS38	pDS132 carrying the *lac*Z::*dif*G allele flanked by the upstream and downstream regions of *dif*2; Cm^r	This study
pMEV245	pDS132 carrying an *arr*2 cassette flanked by the upstream and downstream region of *V. cholerae* *xer*C; Cm^r, Rf^r	This study
pMEV68	pDS132 carrying the upstream and downstream regions of *V. cholerae* *rec*A; Cm^r	(4)

1. Demarre G, et al. (2005) A new family of mobilizable suicide plasmids based on broad host range R388 plasmid (IncW) and RP4 plasmid (IncPalpha) conjugative machineries and their cognate *Escherichia coli* host strains. *Res Microbiol* 156:245–255.
2. Philippe N, Alcaraz JP, Coursange E, Geiselmann J, Schneider D (2004) Improvement of pCVD442, a suicide plasmid for gene allele exchange in bacteria. *Plasmid* 51:246–255.
3. Skorupski K, Taylor RK (1996) Positive selection vectors for allelic exchange. *Gene* 169:47–52.
4. Val M-E, et al. (2008) FtsK-dependent dimer resolution on multiple chromosomes in the pathogen Vibrio cholerae. *PLoS Genet* 4:e1000201.

Table S3. *dif*1 integration of CTXϕ in *recA*$^-$ and *xerC*$^-$ strains

Phage machinery	*att*P sequence	Host machinery	% Integration	Screened colonies
El Tor	El Tor	*recA*$^-$	100.0	180
El Tor	El Tor	*xerC*$^-$	<0.5	183
Classical	Classical	*recA*$^-$	47.4	76
Classical	Classical	*xerC*$^-$	<0.2	550

Table S4. The category of the *att*P attachment region of various CTXϕ variants

Phage origin	*att*P category
VC44RS1J2E	El Tor
AB299799	El Tor
VC44RS1J1E	El Tor
N16961	El Tor
O139AY101180	El Tor
VCU83796	El Tor
AF510994	Classical
AF175708	Classical
AY349175	Classical
DQ012295	Classical
O395LRS2C	Classical
O395SRS2C	Classical
AF110029	Classical
AF238372	Classical
AF30279	G
AF416590	G

Table S5. Oligonucleotides used in this study

Name	Sequence
Dif1top	5′ATCAGTGCGCATTATGTATGTTATGTTAAATGGA
Dif1bot	5′CTGTCCATTTAACATAACATACATAATGCGCACTGAT
Dif2top	5′ATCAATGCGCATTACGTGCGTTATGTTAAATGGA
Dif2bot	5′CTGTCCATTTAACATAACGCACGTAATGCGCATTGAT
DifGtop	5′ATCAGTGCGCATTAGGTATATTATGTTAAATGGA
DifGbot	5′CTGTCCATTTAACATAATATACCTAATGCGCACTGAT
AttPdif1top	5′TACGCCCTTAGTGCGTATTATGTGGCGCGGCATTATGTTGAGGGTTCCG
AttPdif1bot	5′CTGCGGAACCCGTAACATAATGGCGTATAATACGCATTAAGGGCGTA
AttPmutClbot	5′CTGCGGAACCCGTAACATAATGGCGAGTAATACGCATTAAGGGCGTA
AttPmuCltop	5′TACGCCCTTAGTGCGTATTACGTGGCGCGGCATTATGTTGAGGGTTCCG
AttPGtop	5′TACGCCCTTAGTGCGTATTAGGTGGTGCGGCATTATGTTGAGGGTTCCG
AttPGbot	5′CTGCGGAACCCGTAACATAATGCCCCTAATACGCATTAAGGGCGTA
Dif2topextended	5′TAATCTAGATTATGCCTTAATTTAACATAACGCACGTAATGCGCATTAAGTGTTCGTAGGTCGACGAT
Dif2botextended	5′ATCGTCGACCTACGAACACTTAATGCGCATTACGTGCGTTATGTTAAATTAAGGCATAATCTAGATTA
DifGtopextended	5′CAATCTAGACCGCCGCCTTAGTGCGCATTAGGTATATTATGTTAAATTAAGGCATAATGTCGACAA
DifGbotextended	5′TTGTCGACATTATGCCTTAATTTAACATAATATACCTAATGCGCACTAAGGCGGCGGTCTAGATTG
Dif1topextended	5′CAATCTAGACCGCCGCCTTAGTGCGCATTATGTATGTTATGTTAAATTAAGGCATAATGTCGACAA
Dif1botextended	5′TTGTCGACATTATGCCTTAATTTAACATAACATACATAATGCGCACTAAGGCGGCGGTCTAGATTG

Table S6. Sequence of *dif*1 in different CTXϕ-negative strains

Strain	Serotype	*dif*1 sequence	CTX	Sources
N16961	O1 (ET)	AGTGCGTATTA TGTATG TTATGTTAAAT	+	(1)
O395	O1 (Cl)	AATGCGTATTA CGTGCG TTATGTTAAAT	+	CP000626.1
H25	O1 (ET)	AGTGCGTATTA GGTATA TTATGTTAAAT	–	This study
H12	O1 (ET)	AGTGCGTATTA GGTATA TTATGTTAAAT	–	This study
WO5	O1 (ET)	AGTGCGTATTA GGTATA TTATGTTAAAT	–	This study
Ku-40	O1 (ET)	AGTGCGTATTA GGTATA TTATGTTAAAT	–	AY368493.1
93333	O139	AGTGCGTATTA GGTATA TTATGTTAAAT	–	AY368494.1
AM19226	Non O1/ non O139	AGTGCGTATTA GGTATA TTATGTTAAAA	–	(2)
1587	Non O1/ non O139	AGTGCGTATTA GGTATA TTATGTTAAAT	–	(2)
RC385	Non O1/ non O139	AGTGCGTATTA GGTGTA TTATGTTAAAA	–	(2)

1. Val M-E, et al. (2008) FtsK-dependent dimer resolution on multiple chromosomes in the pathogen *Vibrio cholerae*. *PLoS Genet* 4:e1000201.
2. Faruque SM, et al. (2007) Genomic analysis of the Mozambique strain of *Vibrio cholerae* O1 reveals the origin of El Tor strains carrying classical CTX prophage. *Proc Natl Acad Sci USA* 104:5151–5156.

Table S7. *dif*G integration of CTXϕ on the second chromosome of V. *cholerae*

Phage machinery	*att*P sequence	*dif* sequence	% integration	Number of screened colonies
El Tor	El Tor	*dif*G	<0.2	625
Classic	Classic	*dif*G	<0.1	1526
El Tor	G	*dif*G	2.2	1598